Delay-Induced Oscillations in a Logistic–Allee Model with Harvesting

Tian, Jie
University of Nevada, Reno
jtian@unr.edu

Document updated: February 23, 2026

Abstract

This paper examines the stability properties of a delayed logistic–Allee model with harvesting. We begin by reviewing the fundamental concepts of equilibrium points, linear stability, characteristic equations for delay differential equations, and Hopf bifurcation. The model is then reformulated as an equivalent ODE system, from which we derive the characteristic equation and analyze how eigenvalues determine local stability. Our results identify the parameter conditions under which a Hopf bifurcation arises, marking the transition from steady-state behavior to oscillatory dynamics. These findings provide the theoretical groundwork for understanding delay-induced instability in population models.

1 Introduction

Ordinary differential equation (ODE) models are fundamental tools for describing population dynamics, ecological interactions, and numerous biological processes.

Classical logistic growth captures the self-limiting nature of populations due to density dependence, while the Allee effect characterizes reduced growth at low population density, often caused by mate limitation or cooperative behavior. Combining these mechanisms allows researchers to analyze more realistic population dynamics, particularly when extinction thresholds or multiple equilibria may arise.

In many real biological systems, however, population growth does not respond instantaneously to current density levels. Maturation time, gestation delay, and time-lagged resource availability can introduce significant delays into the regulation of population change. Delays are well known to induce oscillatory dynamics in population models, and even simple single-species systems may undergo stability switches and Hopf bifurcations when delayed feedback is present [Kuang (1993); Hassard et al. (1981)].

Such phenomena have motivated extensive study of delay differential equations (DDEs), which frequently exhibit rich dynamical behavior such as oscillations, stability switches, and delay-induced bifurcations. Incorporating harvesting further complicates the system by adding external pressure that may shift equilibria or destabilize previously stable states.

For populations exhibiting Allee effects, delayed density dependence interacts strongly with harvesting and can critically shape persistence thresholds [Berec et al. (2007)], motivating a careful analysis of stability boundaries. To approximate discrete delays, Erlang or gamma-chain constructions offer a finite-dimensional representation that typically preserves the qualitative behavior of the underlying delay equation while enabling efficient numerical exploration [Smith (2011)].

Motivated by these considerations, we study a delayed logistic–Allee model with constant harvesting. Specifically, we consider a delayed logistic-Allee model with constant harvesting, that is

$$\dot{x}(t) = r\,x(t)\left(1 - \frac{x(t-\tau)}{K}\right)\left(\frac{x(t-\tau)}{A} - 1\right) - h,$$

where $x(t)$ represents the population density at time t, $r > 0$ is the intrinsic growth rate, $K > 0$ denotes the environmental carrying capacity, and $A > 0$ is the is the Allee threshold below which the polulation expreience negative growth. The delay parameter $\tau > 0$ models the time lag in reprodcution or environmental feedback. The constant term $h > 0$ represents a constant harvesting rate, accoundting for the continuous removal of individuals from the population due to human exploitation or natural predation.

This model actually is a delay differential equation (DDE) because the rate of change of the current state $\dot{x}(t)$ depends not only on the present value $x(t)$, but aslo on a past state $x(t-\tau)$. In this work, also study how the Hopf threshold depends on the Erlang-chain length k, demonstrating that the critical delay converges rapidly as k increases.

1.1 Research Goal and Questions

The goal of this study is to analyze the local stability of equilibria and to determine whether delay-induced Hopf bifurcations occur as the parameter τ varies. In particular, we aim to identify parameter regimes where small delays preserve stability, as well as regimes where sufficiently large delays produce sustained oscillations through Hopf bifurcation. These results help clarify the interplay between density-dependent growth, delayed feedback, and harvesting, providing insight into long-term population persistence under realistic ecological conditions.

This model extends the classical logistic and Allee models by incorporating both time delay and harvesting, two key ecological factors that can significantly influence population stability and persistence. As the delay τ increases, the system may lose stability through a Hopf bifurcation, leading to oscillatory population dynamics.

- How does the introduction of delay τ change system stability?

- Does a Hopf bifurcation occur as τ increases? If it does, we have a τ_c, how it will change if we change k?
- What are the biological implications of delay-induced oscillations?

1.2 Approach/Methods

[Hurtado and Richards (2020)] introduced a new $GLCT$-based procedure that can be used to quickly formulated new ODE models that explictly incorporate phase-type distributed dalays. Briefly speaking, consider an equation of the form

$$\frac{d}{dt}x(t) = f(x(t), x(t-\tau)) \tag{1}$$

with solution $x(t)$ that includes the initial data over $[-\tau, 0]$ given by $x(t) = \phi(t)$, $t \in [-\tau, 0]$,

we may write down a system of ODEs that approximates equation (1) and it can be approximated by

$$\begin{cases} \frac{d}{dt}x_0(t) = f(x_0(t), x_k(t)) \\ \frac{d}{dt}x_i(t) = \frac{k}{\tau}[x_{i-1}(t) - x_i(t)], i = 1, \cdots, k \end{cases} \tag{2}$$

with initial conditions $x_i(0) = \phi(-\tau i/k)$ for $i = 0, 1, \cdots, k$. Next, we can use this ODE system to analyze the equilibrium points and bifurcation structure of the original model.

2 Results

Before analyzing the stability and bifurcation structure of the system, we first review the relevant definitions and introduce several foundational results from stability and bifurcation theory.

2.1 preliminary

Definition 2.1 (Equilibrium point)**.** Consider a dynamical system

$$\dot{x} = f(x), \qquad x \in \mathbb{R}^n.$$

A point $x^* \in \mathbb{R}^n$ is called an *equilibrium point* if it satisfies

$$f(x^*) = 0.$$

Definition 2.2 (Linear stability of an equilibrium)**.** Consider the dynamical system

$$\dot{x} = f(x), \qquad x \in \mathbb{R}^n,$$

and let x^* be an equilibrium point. Let $A = Df(x^*)$ denote the Jacobian matrix evaluated at x^*.

- The equilibrium x^* is called *(locally) asymptotically stable* if all eigenvalues of A satisfy

$$\Re(\lambda_j) < 0 \qquad \text{for all } j.$$

- The equilibrium x^* is called *unstable* if at least one eigenvalue of A satisfies

$$\Re(\lambda_j) > 0.$$

Now, let us consider Hopf bifurcation.

Definition 2.3 (Hopf bifurcation [Strogatz (2014)).] Consider a smooth one-parameter family of dynamical systems

$$\dot{x} = f(x, \mu), \qquad x \in \mathbb{R}^n,\ \mu \in \mathbb{R}.$$

An equilibrium point (x^*, μ_0) undergoes a *Hopf bifurcation* if the following conditions are satisfied. First, the equilibrium exists, that is,

$$f(x^*, \mu_0) = 0.$$

Next, the Jacobian matrix $Df(x^*, \mu_0)$ possesses a simple conjugate pair of purely imaginary eigenvalues

$$\lambda_{1,2}(\mu_0) = \pm i\omega_0, \qquad \omega_0 > 0,$$

while all remaining eigenvalues have nonzero real part. In addition, the eigenvalue pair crosses the imaginary axis with nonzero speed,

$$\frac{d}{d\mu}\Re(\lambda_{1,2}(\mu))\Big|_{\mu=\mu_0} \neq 0.$$

Under these hypotheses, the equilibrium changes stability as μ passes through μ_0 and a branch of periodic solutions is locally created or destroyed.

Guckenheimer et al. (1997) showed a sufficient condition for $J = Df(x^*, \mu_0)$ has precisely one pair of pure imaginary eigenvalues. Denote the characteristic polynomial of J by

$$p(\lambda) = c_0 + c_1\lambda + \cdots + c_{n-1}\lambda^{n-1} + \lambda^n.$$

Theorem 2.4. *[Guckenheimer et al. (1997)] J has precisely one pair of pure imaginary eigenvalues if*

$$\det(S) = 0 \qquad \textit{and} \qquad \det(S_0)\,\det(S_1) > 0.$$

If $\det(S) \neq 0$ *or* $\det(S_0)\,\det(S_1) < 0$*, then* $p(\lambda)$ *has no purely imaginary roots.*

where

Case 1: n **is even.** Then $\mathcal{S}$ is the $(n-1)\times(n-1)$ matrix

$$\mathcal{S}=\begin{bmatrix} c_0 & c_2 & \cdots & c_{n-2} & 1 & 0 & 0 & \cdots & 0 \\ 0 & c_0 & c_2 & \cdots & c_{n-2} & 1 & 0 & \cdots & 0 \\ \vdots & & \ddots & & & \vdots & & & \vdots \\ 0 & \cdots & \cdots & 0 & c_0 & c_2 & \cdots & c_{n-2} & 1 \\ c_1 & c_3 & \cdots & c_{n-1} & 0 & 0 & \cdots & \cdots & 0 \\ 0 & c_1 & c_3 & \cdots & c_{n-1} & 0 & \cdots & \cdots & 0 \\ \vdots & & \ddots & & & \vdots & & & \vdots \\ 0 & \cdots & \cdots & 0 & c_1 & c_3 & \cdots & \cdots & c_{n-1} \end{bmatrix},$$

with

$$\frac{n-2}{2} \text{ rows of the first block,} \qquad \frac{n}{2} \text{ rows of the second block.}$$

S_i, $i=0,1$, denoted the matrix obtained from $\mathcal{S}$ by deleting the rows 1 and $\frac{n}{2}$ and deleting the columns 1 and $i+2$.

$$S_0=\begin{bmatrix} c_2 & c_4 & \cdots & c_{n-2} & 1 & 0 & \cdots & \cdots & 0 \\ c_0 & c_2 & \ddots & c_{n-4} & c_{n-2} & 1 & 0 & \cdots & 0 \\ 0 & c_0 & \ddots & \ddots & c_{n-4} & c_{n-2} & 1 & \cdots & 0 \\ \vdots & \vdots & \ddots & \ddots & \ddots & \ddots & \ddots & \ddots & \vdots \\ 0 & 0 & \cdots & c_0 & c_2 & \cdots & \cdots & c_{n-2} & 1 \\ c_3 & c_5 & \cdots & c_{n-1} & 0 & 0 & \cdots & \cdots & 0 \\ c_1 & c_3 & \ddots & c_{n-3} & c_{n-1} & 0 & \cdots & \cdots & 0 \\ 0 & c_1 & \ddots & \ddots & c_{n-3} & c_{n-1} & \cdots & \cdots & 0 \\ \vdots & \ddots & \ddots & \ddots & \ddots & \ddots & \ddots & \ddots & \vdots \\ 0 & 0 & \cdots & c_1 & c_3 & c_5 & \cdots & \cdots & c_{n-1} \end{bmatrix},$$

and

$$S_1=\begin{bmatrix} c_0 & c_4 & \cdots & c_{n-2} & 1 & 0 & \cdots & \cdots & 0 \\ 0 & c_2 & \ddots & c_{n-4} & c_{n-2} & 1 & 0 & \cdots & 0 \\ 0 & c_0 & \ddots & \ddots & c_{n-4} & c_{n-2} & 1 & \cdots & 0 \\ \vdots & \vdots & \ddots & \ddots & \ddots & \ddots & \ddots & \ddots & \vdots \\ 0 & 0 & \cdots & c_0 & c_2 & \cdots & \cdots & c_{n-2} & 1 \\ c_1 & c_5 & \cdots & c_{n-1} & 0 & 0 & \cdots & \cdots & 0 \\ 0 & c_3 & \ddots & c_{n-3} & c_{n-1} & 0 & \cdots & \cdots & 0 \\ 0 & c_1 & \ddots & \ddots & c_{n-3} & c_{n-1} & \cdots & \cdots & 0 \\ \vdots & \ddots & \ddots & \ddots & \ddots & \ddots & \ddots & \ddots & \vdots \\ 0 & 0 & \cdots & c_1 & c_3 & c_5 & \cdots & \cdots & c_{n-1} \end{bmatrix},$$

Case 2: n **odd.** Then $\mathcal{S}$ is defined as

$$\mathcal{S} = \begin{bmatrix} c_0 & c_2 & \cdots & c_{n-3} & c_{n-1} & 0 & 0 & \cdots & 0 \\ 0 & c_0 & c_2 & \cdots & c_{n-3} & c_{n-1} & 0 & \cdots & 0 \\ \vdots & & & & & & & & \vdots \\ 0 & \cdots & \cdots & 0 & c_0 & c_2 & \cdots & c_{n-3} & c_{n-1} \\ c_1 & c_3 & \cdots & c_{n-2} & 1 & 0 & \cdots & \cdots & 0 \\ 0 & c_1 & c_3 & \cdots & c_{n-2} & 1 & 0 & \cdots & 0 \\ \vdots & & \ddots & & & \vdots & & & \vdots \\ 0 & \cdots & \cdots & 0 & c_1 & c_3 & \cdots & c_{n-1} & 1 \end{bmatrix},$$

with

$$\frac{n-1}{2} \text{ rows of the first block,} \qquad \frac{n-1}{2} \text{ rows of the second block.}$$

S_i, $i = 0, 1$, denoted the matrix obtained from $\mathcal{S}$ by deleting rows 1 and $\frac{n+1}{2}$ and deleting the columns 1 and $i+2$.

$$S_0 = \begin{bmatrix} c_2 & c_4 & \cdots & c_{n-5} & c_{n-3} & c_{n-1} & 0 & \cdots & 0 \\ c_0 & c_2 & \ddots & c_{n-7} & c_{n-5} & c_{n-3} & c_{n-1} & \ddots & 0 \\ 0 & c_0 & \ddots & \ddots & c_{n-7} & c_{n-5} & c_{n-3} & \ddots & 0 \\ \vdots & \ddots & \ddots & \ddots & \ddots & \ddots & \ddots & \ddots & \vdots \\ 0 & 0 & \cdots & \cdots & c_0 & c_2 & c_4 & \cdots & c_{n-1} \\ c_3 & c_5 & \cdots & c_{n-2} & 1 & 0 & 0 & \cdots & 0 \\ c_1 & c_3 & \cdots & c_{n-4} & c_{n-2} & 1 & 0 & \cdots & 0 \\ 0 & c_1 & \cdots & \ddots & c_{n-4} & c_{n-2} & 1 & \cdots & 0 \\ \vdots & \ddots & \ddots & \ddots & \ddots & \ddots & \ddots & \ddots & \vdots \\ 0 & 0 & \cdots & c_1 & c_3 & c_5 & c_7 & \cdots & 1 \end{bmatrix},$$

and

$$S_1 = \begin{bmatrix} c_0 & c_4 & \cdots & c_{n-5} & c_{n-3} & c_{n-1} & 0 & \cdots & 0 \\ 0 & c_2 & \ddots & c_{n-7} & c_{n-5} & c_{n-3} & c_{n-1} & \ddots & 0 \\ 0 & c_0 & \ddots & \ddots & c_{n-7} & c_{n-5} & c_{n-3} & \ddots & 0 \\ \vdots & \ddots & \ddots & \ddots & \ddots & \ddots & \ddots & \ddots & \vdots \\ 0 & 0 & \cdots & \cdots & c_0 & c_2 & c_4 & \cdots & c_{n-1} \\ c_1 & c_5 & \cdots & c_{n-2} & 1 & 0 & 0 & \cdots & 0 \\ 0 & c_3 & \cdots & c_{n-4} & c_{n-2} & 1 & 0 & \cdots & 0 \\ 0 & c_1 & \cdots & \ddots & c_{n-4} & c_{n-2} & 1 & \cdots & 0 \\ \vdots & \ddots & \ddots & \ddots & \ddots & \ddots & \ddots & \ddots & \vdots \\ 0 & 0 & \cdots & c_1 & c_3 & c_5 & c_7 & \cdots & 1 \end{bmatrix},$$

For some smaller n,

n	$\det S$
	$\det(S_0) \cdot \det(S_1)$
2	c_1
	c_0
3	$c_0 - c_1c_2$
	c_1
4	$c_0c_3^2 - c_1c_2c_3 + c_1^2$
	c_1c_3
5	$(c_2 - c_3c_4)(c_1c_2 - c_0c_3) + c_1c_4(c_1c_4 - 2c_0) + c_0^2$
	$(c_2 - c_3c_4)(c_0 - c_1c_4)$
6	$c_0c_5^2(c_0c_5 - c_2c_3) + c_1c_5^2(c_2^2 - c_0c_4) + c_1(c_1^2 + c_0c_3c_5)$ $+c_1c_5(c_0c_3 - 2c_1c_2) + (c_4c_5 - c_3)(c_0c_3^2 - c_0c_1c_5 + c_1^2c_4 - c_1c_2c_3)$
	$(c_1c_3 + c_0c_5^2 - c_1c_4c_5)(c_3^2 - c_1c_5 + c_2c_5^2 - c_3c_4c_5)$

Table 1: Expressions of $\mathcal{R}_s = \det(S_0)\det(S_1)$ for small n

2.2 Reduction to an ODE System and Derivation of the Characteristic Equation

Based on the method we mensioned in Section 1.2, we can transform the equation

$$\dot{x}(t) = r\,x(t)\left(1 - \frac{x(t-\tau)}{K}\right)\left(\frac{x(t-\tau)}{A} - 1\right) - h,$$

into that is

$$\dot{x}_0(t) = f(x_0(t), x_k(t)) = r x_0(t)(1 - \frac{x_k(t)}{K})(\frac{x_k(t)}{A} - 1) - h \tag{3a}$$

$$\dot{x}_1(t) = \frac{k}{\tau}[x_0(t) - x_1(t)] \tag{3b}$$

$$\dot{x}_2(t) = \frac{k}{\tau}[x_1(t) - x_2(t)] \tag{3c}$$

$$\ddots \tag{3d}$$

$$\dot{x}_k(t) = \frac{k}{\tau}[x_{k-1}(t) - x_k(t)] \tag{3e}$$

$$x_i(0) = \phi(-\tau i/k), \text{ for } i = 0, 1, \cdots, k \tag{3f}$$

The equations for x_i, $i = 1, \cdots, n$ in System (3) can be written in matrix form,

$$\dot{x}_0(t) = f(x_0(t), x_k(t))$$
$$\frac{d\mathbf{x}(t)}{dt} = \mu x_0 v + M^T \mathbf{x}$$

where $\mathbf{x} = [x_1, \cdots, x_n]^T$, $x_i(0) = \phi(-\tau i/k)$, for $i = 0, 1, \cdots, k$,

$$v = \begin{bmatrix} 1 \\ 0 \\ \vdots \\ 0 \end{bmatrix} \text{ and } M = \begin{bmatrix} -\mu & \mu & 0 & \cdots & 0 \\ 0 & -\mu & \mu & \ddots & 0 \\ \vdots & \ddots & \ddots & \ddots & \ddots \\ 0 & 0 & \ddots & -\mu & \mu \\ 0 & 0 & \cdots & 0 & -\mu \end{bmatrix}, \ \mu = \frac{k}{\tau}.$$

Consider the ODEs in (3), any equilibrium must satisfy $x_0 = \cdots = x_k = x^*$ with

$$r\,x^*\left(1 - \tfrac{x^*}{K}\right)\left(\tfrac{x^*}{A} - 1\right) - h = 0. \tag{5}$$

Equation (5) is a cubic in x^* and depending on (r, K, A, h). It admits one to three real roots, of which biologically meaningful equilibria require $x^* > 0$.

Let $f(x_0, x_k) := r\,x_0(1 - \frac{x_k}{K})(\frac{x_k}{A} - 1) - h$. At an equilibrium $(x^*, \ldots, x^*)$, the partial derivatives are

$$f_{x_0}\big|_{x_*} \;=\; r\left(1 - \tfrac{x^*}{K}\right)\left(\tfrac{x^*}{A} - 1\right) =: \alpha,$$

$$f_{x_k}\big|_{x_*} \;=\; r\,x^*\Big[-\tfrac{1}{K}\Big(\tfrac{x^*}{A}-1\Big)+\Big(1-\tfrac{x^*}{K}\Big)\tfrac{1}{A}\Big] = r\,x^*\big(\tfrac{1}{A}+\tfrac{1}{K}-\tfrac{2x^*}{AK}\big) =: \beta.$$

Thus the $(k{+}1)\times(k{+}1)$ Jacobian matrix at $(x^*,\ldots,x^*)$ is

$$J(x^*) \;=\; \begin{bmatrix} \alpha & 0 & 0 & \cdots & 0 & \beta \\ \mu & -\mu & 0 & \cdots & 0 & 0 \\ 0 & \mu & -\mu & \cdots & 0 & 0 \\ \vdots & & \ddots & \ddots & \vdots & \vdots \\ 0 & \cdots & 0 & \mu & -\mu & 0 \\ 0 & \cdots & 0 & 0 & \mu & -\mu \end{bmatrix}. \tag{6}$$

The characteristic equation of (6) is

$$(\lambda-\alpha)(\lambda+\mu)^k \;=\; \beta\,\mu^k \tag{7}$$

Equaivalently,

$$\lambda = \alpha + \beta(\frac{\mu}{\lambda+\mu})^k \tag{8}$$

As $k\to\infty$ with $\mu = k/\tau$, one has $\big(\frac{\mu}{\lambda+\mu}\big)^k \to e^{-\lambda\tau}$, so (7) tends to the DDE characteristic equation $\lambda = \alpha + \beta e^{-\lambda\tau}$.

We start from the characteristic equation

$$p(\lambda) = (\lambda-\alpha)(\lambda+\mu)^k - \beta\,\mu^k.$$

Now, we proceed by studying the characteristic equation from two separate but related perspectives.

2.2.1 Eigenvalues that satisfies the definition of Hopf bifurcation

First, let $\lambda = i\omega$ with $\omega\neq 0$ and $\mu = k/\tau$. Write

$$\left(\frac{\mu}{i\omega+\mu}\right)^k = \left(\frac{\mu}{\sqrt{\mu^2+\omega^2}}\right)^k \exp\Big(-i\,k\,\arctan\tfrac{\omega}{\mu}\Big).$$

Splitting real/imag parts in (8) yields the Hopf equations

$$0 \;=\; \alpha \;+\; \beta\left(\frac{\mu}{\sqrt{\mu^2+\omega^2}}\right)^k \cos\Big(k\,\arctan\tfrac{\omega}{\mu}\Big), \tag{9}$$

$$\omega \;=\; -\,\beta\left(\frac{\mu}{\sqrt{\mu^2+\omega^2}}\right)^k \sin\Big(k\,\arctan\tfrac{\omega}{\mu}\Big). \tag{10}$$

A Hopf bifurcation occurs at parameter values (τ, r, K, A, h) for which (9)–(10) admit a solution (ω, μ) with $\omega \neq 0$, and the standard transversality condition holds:

$$\frac{d}{d\tau} \operatorname{Re} \lambda(\tau)\Big|_{\tau=\tau_c} \neq 0.$$

In practice, fix an equilibrium x^* via (5), compute (α, β), then solve (9)–(10) for (ω, μ) to obtain the critical delay $\tau_c = k/\mu$. The direction and stability of the emerging periodic orbits follow from the usual Hopf normal form calculations for ODEs.

If $\beta = 0$, (8) gives $\lambda = \alpha$, so no delay-induced oscillation arises from the chain. For $k = 1$ (exponential delay), (7) simplifies to $(\lambda - \alpha)(\lambda + \mu) = \beta\mu$ and can be analyzed explicitly.

2.2.2 Gucakenheimer‘s method

Let us consider the characteristic equation, and expand it, we can see that

$$(\lambda + \mu)^k = \sum_{j=0}^{k} \binom{k}{j} \mu^{k-j} \lambda^j.$$

Then, we can rewrite the characteristic equation,

$$p(\lambda) = \lambda \sum_{j=0}^{k} \binom{k}{j} \mu^{k-j} \lambda^j - \alpha \sum_{j=0}^{k} \binom{k}{j} \mu^{k-j} \lambda^j - \beta\mu^k.$$

Thus

$$p(\lambda) = \sum_{j=0}^{k} \binom{k}{j} \mu^{k-j} \lambda^{j+1} - \alpha \sum_{j=0}^{k} \binom{k}{j} \mu^{k-j} \lambda^j - \beta\mu^k.$$

We now collect the coefficients of equal powers of λ. The polynomial has degree $k + 1$, and may be written as

$$p(\lambda) = c_0 + c_1\lambda + \cdots + c_k\lambda^k + \lambda^{k+1}.$$

Thus,

$$c_0 = -(\alpha + \beta)\mu^k, \qquad c_j = \mu^{k-j}\Big[\binom{k}{j-1}\mu - \alpha\binom{k}{j}\Big], \quad 1 \leq j \leq k. \tag{11}$$

Now, using the Theorem 2.4, we can determine the values of τ for which a Hopf bifurcation occurs.

For different k, k=1,2,3, by (11) and Theorem 2.4, we can get

$k = 1 \Rightarrow n = 2$

$$c_0 = -(\alpha + \beta)\mu,$$
$$c_1 = \mu - \alpha.$$

$k = 2 \Rightarrow n = 3$

$$
\begin{aligned}
c_0 &= -(\alpha+\beta)\mu^2, \\
c_1 &= \mu^2 - 2\alpha\mu, \\
c_2 &= 2\mu - \alpha.
\end{aligned}
$$

$k = 3 \Rightarrow n = 4$

$$
\begin{aligned}
c_0 &= -(\alpha+\beta)\mu^3, \\
c_1 &= \mu^3 - 3\alpha\mu^2, \\
c_2 &= 3\mu^2 - 3\alpha\mu, \\
c_3 &= 3\mu - \alpha.
\end{aligned}
$$

k	$\det S$ $\det(S_0) \cdot \det(S_1)$
1	$c_1 = \mu - \alpha.$ $c_0 = -(\alpha+\beta)\mu$,
2	$c_0 - c_1 c_2 = -(\alpha+\beta)\mu^2 - (\mu^2 - 2\alpha\mu)(2\mu - \alpha.)$ $\mu^2 - 2\alpha\mu$
3	$c_0 c_3^2 - c_1 c_2 c_3 + c_1^2 = -(\alpha+\beta)\mu^3 - (3\mu-\alpha)^2 - (\mu^3 - 3\alpha\mu^2)(3\mu^2 - 3\alpha\mu)(3\mu - \alpha) + (\mu^3 - 3\alpha\mu^2)^2$ $c_1 c_3 = (\mu^3 - 3\alpha\mu^2)(3\mu - \alpha)$
$\vdots$	$\vdots$

Table 2: Parameter sets associated with bifurcation for $k = 1, 2, 3$

For higher k, take Theorem 2.4 as reference.

3 Numerical verification

To illustrate the delay–induced stability transition of the logistic–Allee model, we combine two complementary diagnostics: (i) the spectral abscissa of the Erlang–chain Jacobian $J(\tau)$, and (ii) Sylvester–type determinants constructed from the characteristic polynomial of $J(\tau)$.

We performed a numerical stability scan and direct time–domain simulations using the parameters

$$r = 1.0, \qquad K = 1.0, \qquad A = 0.3, \qquad h = 0.02, \qquad k = 8.$$

Solving the equilibrium condition

$$rx^* \left(1 - \frac{x^*}{K}\right) \left(\frac{x^*}{A} - 1\right) - h = 0$$

yields three real roots

$$x_1^* = -0.0185, \qquad x_2^* = 0.3273, \qquad x_3^* = 0.9912.$$

The largest positive equilibrium x_3^* is biologically meaningful and is selected for stability analysis.

At $(x^*, x^*) = (0.9912,\, 0.9912)$, the linearization coefficients are

$$\alpha = f_{x_0}(x^*, x^*) = 0.02018, \qquad \beta = f_{x_k}(x^*, x^*) = -2.2550.$$

Substituting these values into the Jacobian matrix

$$J(x^*) = \begin{pmatrix} \alpha & 0 & \cdots & 0 & \beta \\ \mu & -\mu & 0 & \cdots & 0 \\ 0 & \mu & -\mu & \cdots & 0 \\ \vdots & \ddots & \ddots & \ddots & \vdots \\ 0 & \cdots & 0 & \mu & -\mu \end{pmatrix}, \qquad \mu = \frac{k}{\tau},$$

we computed the dominant eigenvalue $\lambda_{\max}$ as a function of τ. Figure 1–3 shows that

$$\tau_c \approx 0.817,$$

indicating the onset of a Hopf bifurcation.

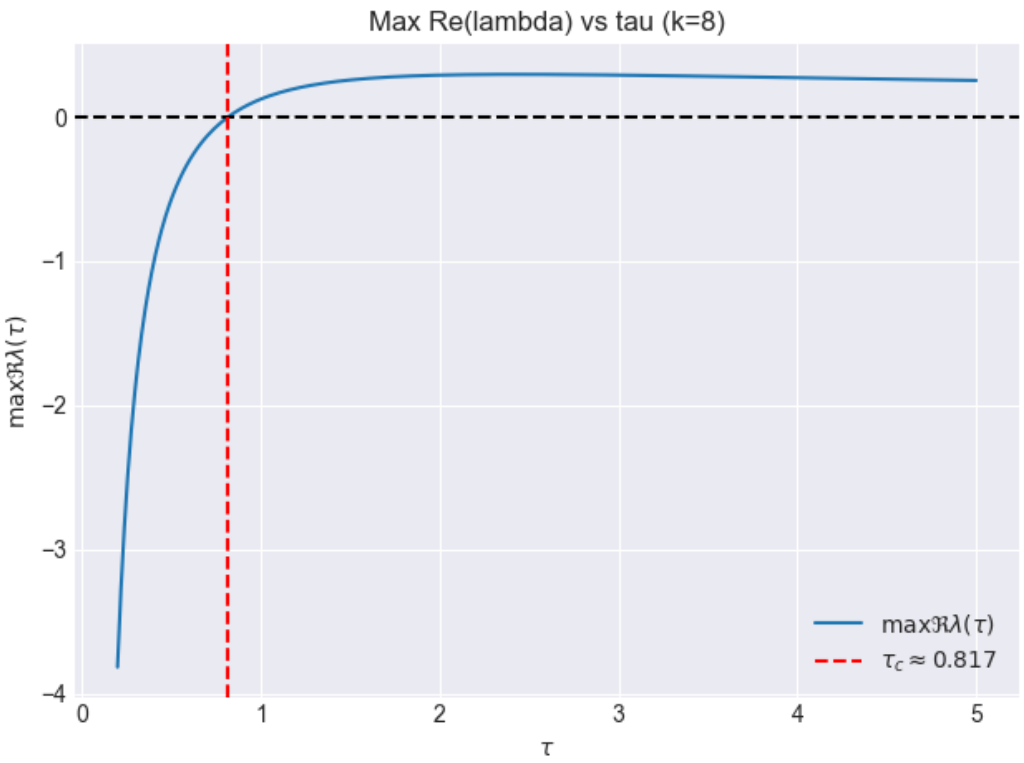


Figure 1: Maximal real part of the eigenvalues of the Erlang–chain Jacobian $J(\tau)$. The curve $\tau \mapsto \max \Re\lambda(\tau)$ is negative for small τ, indicating local asymptotic stability of the equilibrium. As τ increases, a conjugate pair of eigenvalues moves toward the imaginary axis, and the spectral abscissa crosses zero at $\tau = \tau_c \approx 0.817$, marked by the vertical dashed red line. This crossing corresponds to a Hopf bifurcation, where the equilibrium loses stability and a small-amplitude periodic orbit is born.

Remark 3.1. In this setting, $\alpha \neq 0$, so if the real part of an eigenvalue is 0, this eigenvalue must be purely imaginary.

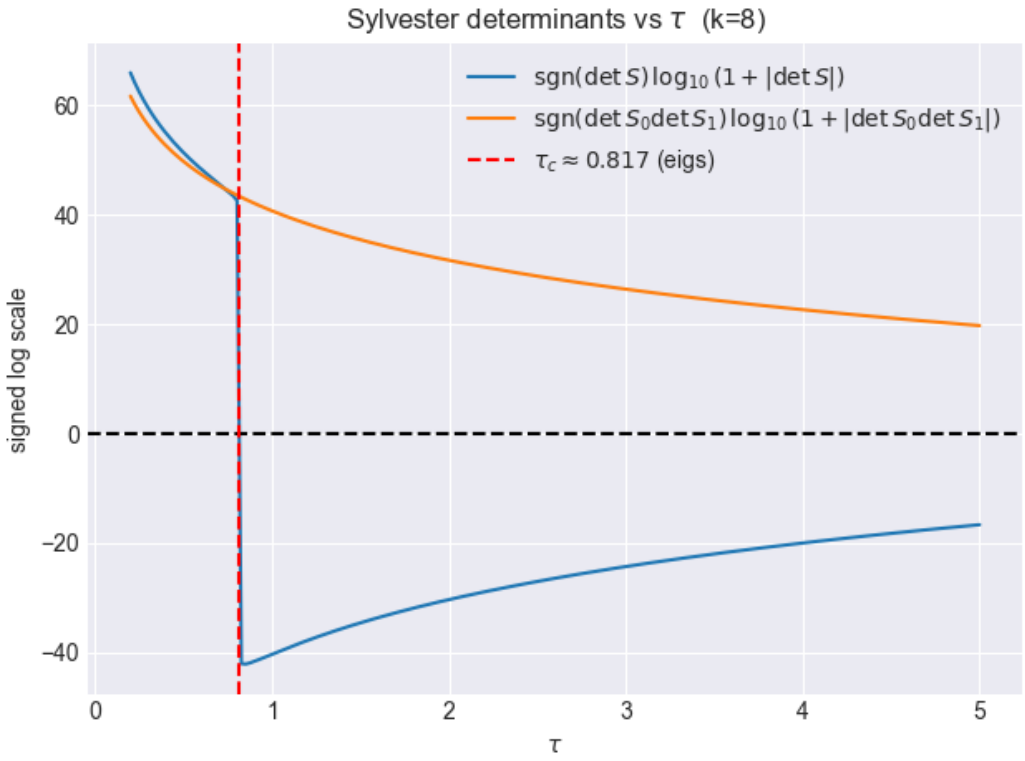


Figure 2: Signed–logarithmic plots of the Sylvester determinant $\det S(\tau)$ and the product $\det S_0(\tau) \det S_1(\tau)$, where S, S_0, S_1 are constructed from the characteristic polynomial of $J(\tau)$ following the criterion of Guckenheimer and Holmes. The transformation $\operatorname{sgn}(x) \log_{10}(1+|x|)$ preserves the sign of each determinant while compressing the enormous magnitudes. A sign change in $\det S(\tau)$ (visible as the blue curve crossing 0) indicates the existence of a purely imaginary root of the characteristic equation. The product $\det S_0(\tau) \det S_1(\tau)$ remains positive near the crossing, verifying the nondegeneracy condition required for a simple Hopf pair. The crossing occurs near the same critical delay $\tau_c \approx 0.817$ identified from the eigenvalue analysis (vertical dashed line).

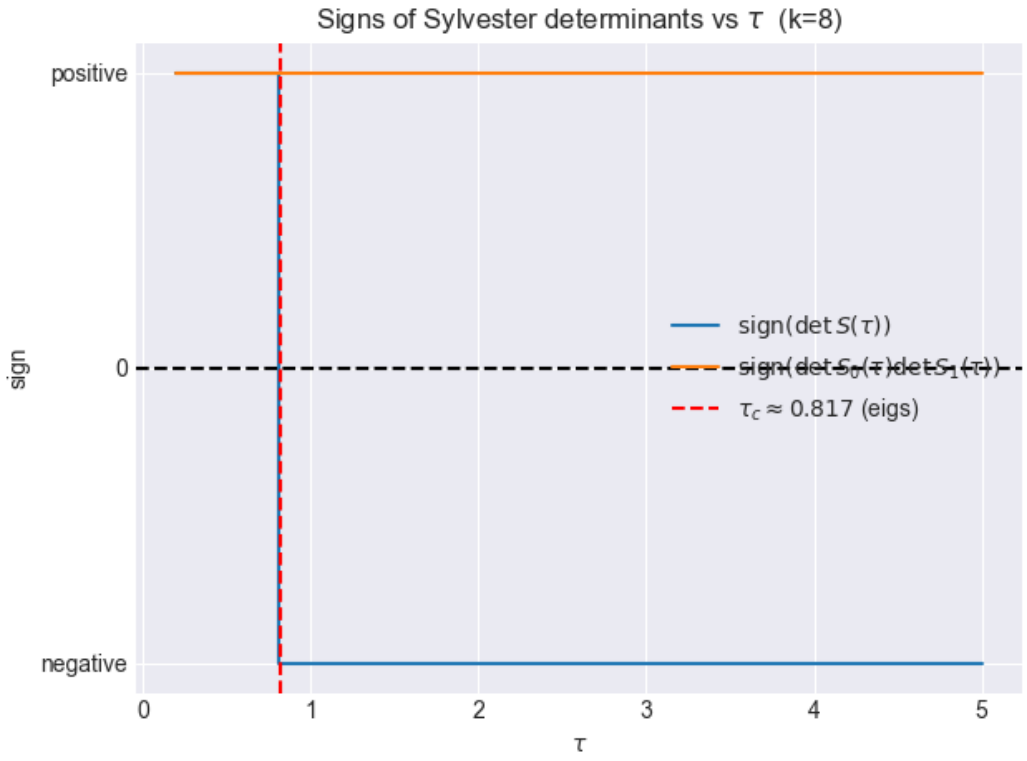


Figure 3: Sign plots of $\det S(\tau)$ and $\det S_0(\tau) \det S_1(\tau)$. This representation makes the qualitative behavior especially transparent: the blue step curve changes sign once, indicating a unique delay value at which $S(\tau)$ becomes singular. At the same value, the orange step curve retains value $+1$, confirming the condition $\det S_0(\tau) \det S_1(\tau) > 0$. Therefore, the Sylvester criterion predicts a Hopf bifurcation at a delay consistent with the eigenvalue crossing in Figure 1.

The numerical evidence presented in Figures 1–3 demonstrates the occurrence of a delay–induced Hopf bifurcation in the logistic–Allee model. Figure 1 shows that the equilibrium is asymptotically stable for small delays, with all eigenvalues of the Erlang–chain Jacobian $J(\tau)$ lying strictly in the left half-plane. As τ increases, a complex conjugate pair approaches the imaginary axis, and the spectral abscissa crosses zero at a critical delay $\tau_c \approx 0.817$. This transition marks the loss of stability and the emergence of a small periodic orbit, characteristic of a Hopf bifurcation.

Figures 2 and 3 provide an independent confirmation of this transition via a Sylvester-type criterion derived from the characteristic polynomial of $J(\tau)$. In Figure 2, the signed–log determinant $\det S(\tau)$ changes sign near the same critical delay, indicating the presence of a purely imaginary root of the characteristic equation. The accompanying product $\det S_0(\tau) \det S_1(\tau)$ remains positive in this region, verifying the nondegeneracy condition required for a simple pair of imaginary eigenvalues. The sign–only plot in Figure 3 further clarifies this behaviour: $\det S(\tau)$ exhibits a single sign jump, while $\det S_0(\tau) \det S_1(\tau)$ stays strictly positive. Thus, the Sylvester test predicts a unique Hopf point, in excellent agreement with the eigenvalue crossing.

Taken together, the eigenvalue analysis and Sylvester determinant tests show that increasing the delay τ destabilizes the positive equilibrium and produces a branch of periodic solutions through a Hopf bifurcation at $\tau = \tau_c$.

In addition, we consider the relationship of k and τ_c. For the parameter set

$$r = 1, \qquad K = 1, \qquad A = 0.3, \qquad h = 0.02,$$

the Logistic–Allee harvesting model admits three equilibria, among which the largest real one is

$$x^* \approx 0.9912433.$$

Linearizing the Erlang-chain approximation with k compartments at x^*, we computed the spectral abscissa $\alpha(\tau; k) = \max \Re\lambda(\tau; k)$ over a dense grid of delay values $\tau \in [0.01, 3]$, and detected the Hopf point as the smallest τ for which $\alpha(\tau; k)$ crosses 0. For $k = 1$ no such crossing occurs in this interval, while for $k \geq 2$ the Hopf crossing is clear and unique (Figure 4).

Table 3 lists the resulting critical delays $\tau_c(k)$. The values decrease monotonically with k:

$$\begin{aligned} &\tau_c(2) = 1.7130, \quad \tau_c(3) = 1.1611, \quad \tau_c(4) = 0.9948, \\ &\tau_c(5) = 0.9153, \quad \tau_c(6) = 0.8689, \quad \tau_c(7) = 0.8384, \quad \tau_c(8) = 0.8169. \end{aligned}$$

Figure 4 shows the decay of $\tau_c(k)$ as a function of k, while Figure 5 plots the same values against $1/k$. Strikingly, the $(1/k, \tau_c)$–relation is almost perfectly linear, and a least-squares fit of the form

$$\tau_c(k) \approx a + \frac{b}{k}$$

gives

$$a = 0.4679936974, \qquad b = 2.3473902518.$$

Hence the Hopf threshold of the exact discrete-delay equation is numerically estimated as

$$\tau_\infty := \lim_{k\to\infty} \tau_c(k) \approx 0.468.$$

These computations demonstrate that: (i) the Erlang approximation preserves the Hopf mechanism of the underlying delay equation; (ii) $\tau_c(k)$ converges rapidly with k; and (iii) the dependence on k is approximately affine in $1/k$. This provides a reliable and systematic way to approximate the true Hopf bifurcation threshold using moderate values of k.

Table 3: Critical delay $\tau_c(k)$ for $k = 1, \ldots, 8$ obtained from the eigenvalue crossing $\max \Re\lambda(\tau; k) = 0$.

k	$\tau_c(k)$
1	— (no crossing on $[0.01, 3]$)
2	1.7130270749
3	1.1610887511
4	0.9948322733
5	0.9153402324
6	0.8688608502
7	0.8383953575
8	0.8168924535

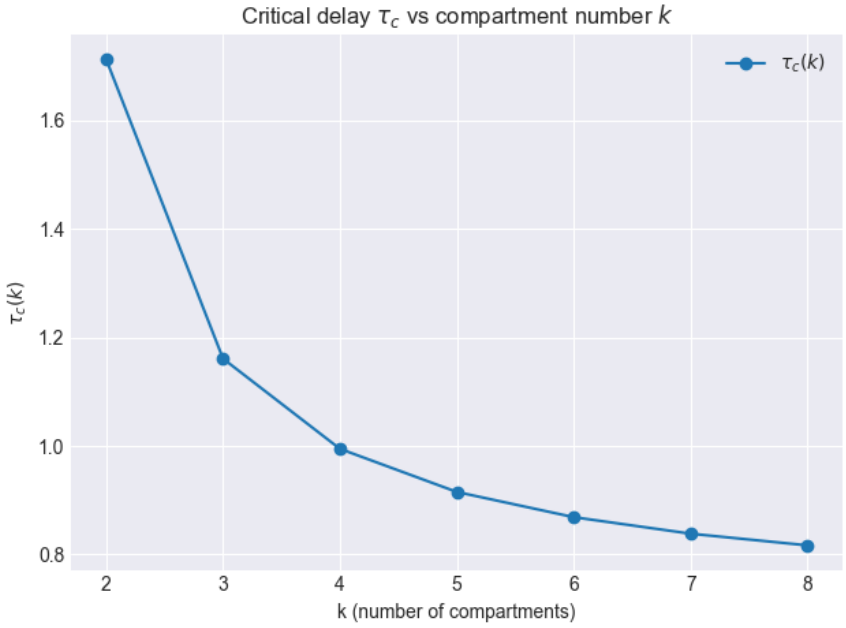


Figure 4: Critical delay $\tau_c(k)$ versus Erlang compartment number k. The curve is strictly decreasing for $k \geq 2$ and stabilizes near $\tau_c \approx 0.82$ for $k = 8$.

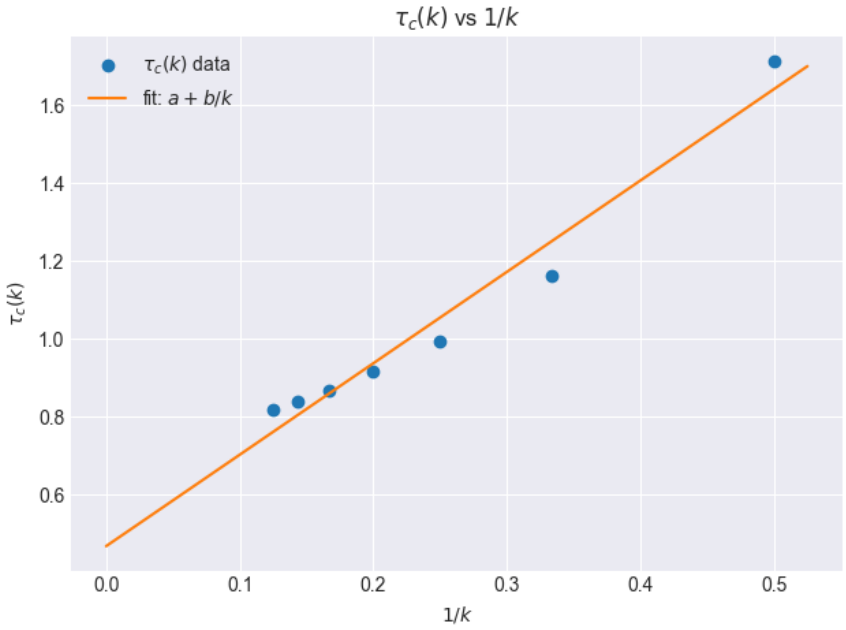


Figure 5: Linear trend of the critical delay when plotted against $1/k$. A least-squares fit of the form $\tau_c(k) \approx a + b/k$ yields $a \approx 0.468$, which numerically approximates the Hopf threshold of the true discrete-delay system.

4 Discussion

1. How does the introduction of delay τ change system stability? The inclusion of a finite delay τ introduces a memory effect into the logistic–Allee model, making the present growth rate depend on past population densities. For sufficiently small τ, the positive equilibrium x^* remains locally asymptotically stable, since all eigenvalues of the Jacobian matrix $J(x^*)$ have negative real parts. As τ increases, the eigenvalues of the characteristic equation gradually approach the imaginary axis. Beyond a critical delay τ_c, one complex-conjugate pair crosses the imaginary axis, causing a loss of stability and the emergence of oscillatory behavior.

2. Does a Hopf bifurcation occur as τ increases? Yes. Using the Erlang-chain approximation, the characteristic equation can be written as

$$(\lambda - \alpha)(\lambda + \tfrac{k}{\tau})^k = \beta\big(\tfrac{k}{\tau}\big)^k,$$

where $\alpha = f_{x_0}(x^*, x^*)$ and $\beta = f_{x_k}(x^*, x^*)$. A Hopf bifurcation occurs when this equation admits purely imaginary roots $\lambda = \pm i\omega_c$, which satisfy

$$\begin{cases} 0 = \alpha + \beta\Big(\frac{\mu}{\sqrt{\mu^2+\omega_c^2}}\Big)^k \cos\Big(k \arctan\frac{\omega_c}{\mu}\Big), \\ \omega_c = -\beta\Big(\frac{\mu}{\sqrt{\mu^2+\omega_c^2}}\Big)^k \sin\Big(k \arctan\frac{\omega_c}{\mu}\Big), \end{cases} \qquad \mu = \tfrac{k}{\tau}.$$

At $\tau = \tau_c = k/\mu_c$, a pair of conjugate eigenvalues crosses the imaginary axis. For $\tau > \tau_c$, $\Re(\lambda) > 0$, and the equilibrium x^* becomes unstable, leading to periodic oscillations of the population density.

3. What are the biological implications of delay-induced oscillations? Delay-induced oscillations imply that time lags in reproduction or environmental feedback can produce sustained population cycles, even under constant environmental and harvesting conditions. Such oscillations correspond to over- and under-shooting of the carrying capacity K due to delayed density regulation. Biologically, this behavior increases extinction risk when the population periodically falls below the Allee threshold A, emphasizing that reproductive delay and harvesting interact as destabilizing ecological forces.

4. How the τ_c changes with respect to k Our computations indicate that the Erlang-chain approximation preserves the Hopf bifurcation structure of the delay equation in a robust and predictable manner. For $k \geq 2$, the critical delay $\tau_c(k)$ decreases monotonically and fits almost perfectly to an affine function of $1/k$, yielding the asymptotic estimate $\tau_\infty \approx 0.468$ for the Hopf threshold of the true discrete-delay model. This demonstrates that even moderate values of k provide an accurate and computationally efficient approximation of the underlying dynamics.

Acknowledgments
I would like to sincerely thank Professor Paul J Hurtado for his guidance, support, and helpful discussions throughout this course. His teaching and feedback have greatly contributed to my understanding and to the completion of this work.

References

Berec, L., E. Angulo, and F. Courchamp. 2007. Multiple allee effects and population management. Trends in Ecology & Evolution 22:185–191.

Guckenheimer, J., M. Myers, and B. Sturmfels. 1997. Computing hopf bifurcations i. SIAM Journal on Numerical Analysis 34:1–21.

Hassard, B. D., N. D. Kazarinoff, and Y.-H. Wan. 1981. Theory and applications of Hopf bifurcation, vol. 41. CUP Archive.

Hurtado, P., and C. Richards. 2020. A procedure for deriving new ode models: Using the generalized linear chain trick to incorporate phase-type distributed delay and dwell time assumptions. Mathematics in Applied Sciences and Engineering 1:412–424.

Kuang, Y. 1993. Delay differential equations: with applications in population dynamics, vol. 191. Academic press.

Smith, H. L. 2011. An introduction to delay differential equations with applications to the life sciences, vol. 57. springer New York.

Strogatz, S. H. 2014. Nonlinear Dynamics and Chaos: With Applications to Physics, Biology, Chemistry, and Engineering. Studies in Nonlinearity, 2nd ed. Westview Press.